Altitude Range and Throughput Analysis for Directional UAV-assisted Backscatter Communications Networks

Zhaoyang WANG, Qiu WANG, Xiangying DANG

The School of Information Engineering, Xuzhou University of Technology, Xuzhou, Jiangsu, China

wangzhaoyang@xzit.edu.cn, qiu_wang@xzit.edu.cn, dangpaper@163.com

Submitted February 12, 2024 / Accepted May 10, 2024 / Online first May 28, 2024

Abstract. *In the realm of Internet of Things (IoT) networks, Backscatter communication (BackCom) is a promising technique that allows devices to send data through the reflecting surrounding radio frequency (RF) signals. Integrating unmanned aerial vehicles (UAVs) with BackCom technology to establish UAV-assisted BackCom networks presents an opportunity to provide self-generated RF signals for backscatter devices, establishing self-sustaining data collection systems. This paper investigates directional UAV-assisted BackCom networks where UAVs are equipped with directional antennas, which differs from previous studies that mainly consider omni-directional antennas. To ensure the quality of BackCom, we develop a theoretical model that analyzes the valid altitude range of UAVs, which is often ignored in previous studies. Based on the altitude range of UAVs, we then derive the throughput of directional UAV-assisted BackCom networks. Extensive simulations are conducted to verify our theoretical model, revealing correlations between the UAV altitude range, the throughput, directional antennas, and other key parameters. Results indicate that UAVs need to set the proper UAV altitude according to multiple parameters to ensure successful communication. In addition, adjusting the beamwidth of directional antennas can enhance both the altitude range of UAVs and the throughput of networks.*

Keywords

Backscatter communications, UAV-assisted networks, directional antennas, altitude range, throughput

1. Introduction

With the rapid expansion of the Internet of Things (IoT) networks, numerous low-power devices are expected to be deployed in smart IoT networks such as smart cities and farms to monitor and gather data to serve a variety of IoT applications [1], [2]. Powering a multitude of devices in such smart networks poses a significant challenge. Backscatter communication (BackCom) is recognized as a promising technology in IoT networks for enabling low-power IoT devices to transmit data by reflecting RF signals with extra-low energy consumption [1]. Furthermore, the integration of unmanned aerial vehicles (UAVs) in data collection processes has been extensively explored due to their flexibility and ease of deployment [3–6]. The combination of UAVs and BackCom forms UAV-assisted BackCom networks, providing self-generated RF signals for backscatter devices (BDs) and establishing sustainable data collection systems [3], [6]. Hence, UAV-assisted BackCom networks have wide applications in smart network scenarios, particularly in remote areas lacking infrastructure for RF signal provision.

Many studies analyze the communication performance of UAV-assisted BackCom networks [3, 4, 6, 7] and the corresponding UAV trajectories [5, 8, 9]. In their analysis, most consider that UAVs fly at a fixed altitude without investigating the valid altitude range of UAVs or investigating the correlation between the UAV altitude and their communication performance [3–9]. However, it is indicated in [10] that the UAV altitude can directly affect the communication coverage in UAV-assisted networks. Moreover, different from common sensor networks, because BackCom needs to experience dual-path transmitting (i.e., receiving signals and reflecting), BackCom is heavily sensitive to communication distance [11]. Additionally, since the activation of BackCom relies on BDs to receive adequate energy, the communication performance of UAV-assisted BackCom networks is far more sensitive to the altitude of UAVs. It is shown in [12] that the altitude of UAVs significantly affects the network throughput of UAV-assisted BackCom networks. Therefore, investigating the UAV altitude range and analyzing how the UAV altitude specifically affects the communication performance of UAV-assisted BackCom networks are crucial for ensuring communication reliability. Althrough omni-directional antennas are usually equipped on UAVs in previous research [3–9], directional antennas are increasingly used in 5G [13] and 6G [14] communication devices. In contrast to omni-directional antennas that uniformly emit/receive signals to/from all directions in a plane, directional antennas can offer targeted signal transmission/reception, enhancing communication efficiency by mitigating dual-path propagation losses in BackCom systems [15], [16]. Consequently, the investigation of directional UAV-assisted BackCom networks is of great significance.

DOI: 10.13164/re.2024.0368

To the best of our knowledge, there is no study exploring how the UAV altitude and directional antennas affect the communication performance of UAV-assisted BackCom networks. Hence, this paper aims to develop an analytical model to investigate the valid UAV altitude range in directional UAV-assisted BackCom networks and evaluate their effect on communication performance. The key contributions of this study are outlined below.

- We identify directional UAV-assisted BackCom networks. Then, we develop a theoretical model to investigate the valid altitude range of UAVs, highlighting the relationship among the altitude range, the beamwidth of directional antennas, and other key parameters.
- We investigate the throughput of directional UAV-assisted BackCom networks, giving the correlation among the throughput, the altitude of UAVs, and the beamwidth of directional antennas.
- Extensive simulations are conducted to verify the theoretical model, revealing correlations between the UAV altitude range, the throughput, the beamwidth of directional antennas, and other key parameters. Results indicate that both the altitude range and the throughput can be increased by decreasing antenna beamwidth.

The rest of this paper is organized as follows. In Sec. 2, we present our system model. In Sec. 3, we analyze the altitude range and the throughput of directional UAV-assisted BackCom networks. Next, Section 4 presents the simulations. At last, Section 5 concludes this paper.

2. System Models

2.1 Network and Antenna Models

As shown in Fig. 1, we focus on a directional UAV-assisted BackCom network consisting of a hovering UAV and numerous BDs. In the network, BDs are distributed according to a homogeneous Poisson point process (HPPP) with a certain density λ_{BD}. Each BD is outfitted with an omni-directional antenna to collect ground data from all directions. Let G_0 represent the gain of omni-directional antennas, where $G_0 = 1$. The radiation pattern of a realistic directional antenna is illustrated in Fig. 2, including a primary lobe and some side lobes [17]. The antenna gain of the directional antenna is varied across different directions. This variability in gain poses challenges when analyzing the performance of directional UAV-assisted BackCom networks. To facilitate analytical tractability, we adopt the sector antenna as our antenna model (depicted in Fig. 2) [18], [19]. The antenna gain of the sector model is constant within the beamwidth θ_{d}. Specifically, the antenna gain of the sector model, denoted by G_{d}, can be shown below [18]:

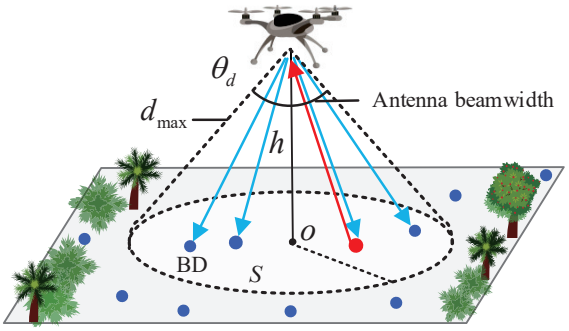

Fig. 1. Example of directional UAV-assisted BackCom networks.

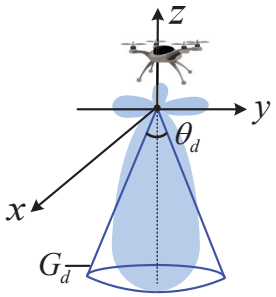

Fig. 2. Example of directional antennas.

$$G_{\mathrm{d}}(\theta) = \begin{cases} \dfrac{2}{1-\cos\left(\frac{\theta_{\mathrm{d}}}{2}\right)} & \theta \in (0,\ \theta_{\mathrm{d}}), \\ 0 & \text{others.} \end{cases} \tag{1}$$

The coverage area of the UAV on the ground, represented by S, can be given by:

$$S = \pi \left(h \tan\left(\theta_{\mathrm{d}}/2\right)\right)^2 = \pi h^2 \tan^2\left(\theta_{\mathrm{d}}/2\right). \tag{2}$$

Meanwhile, the maximum distance from the UAV to BDs within the coverage region of the UAV, expressed by $d_{\max}$, can be calculated as:

$$d_{\max} = \frac{h}{\cos(\theta_{\mathrm{d}}/2)}. \tag{3}$$

The average number of BDs within the coverage region S of a UAV, donated by N, can be determined as follows:

$$N = \lambda_{\mathrm{BD}} \cdot S = \lambda_{\mathrm{BD}} \pi h^2 \tan^2(\theta_{\mathrm{d}}/2). \tag{4}$$

In the process of communications, the time division multiple access (TDMA) [20] is adopted. For a UAV situated at an altitude h, we assume the UAV can establish communications with N BDs within the coverage region by TDMA. Let T_{c} denote the communication time of the BackCom. Then, the communication time T_{c} can be subdivided into N uniform time slots. It is assumed that each BD is assigned a single slot for transmitting data to the UAV.

2.2 Channel Model

The attenuation of each transmission link between a UVA to BDs consists of radio propagation path-loss and small-scale fading. The radio propagation path-loss represented by g_{mix} can be evaluated by the probability mixed of a Line-of-Sight (LoS) condition and a non-Line-of-Sight (NLoS) [10] condition. It is defined as follows [21]:

$$g_{\text{mix}} = 10^{-\left(\frac{P_{\text{LoS}} L_{\text{LoS}} + P_{\text{NLoS}} L_{\text{NLoS}}}{10}\right)} \tag{5}$$

where P_{LoS} and P_{NLoS} are the probability of the LoS condition and the NLoS condition, respectively, given by [21]:

$$P_{\text{LoS}} = \frac{1}{1 + u_1 \exp(-u_2[\theta_z - u_1])}, \tag{6}$$

$$P_{\text{NLoS}} = 1 - P_{\text{LoS}} \tag{7}$$

where u_1 and u_2 are constant geographical surrounding parameters, θ_z denotes the elevation angle from the BD to the UAV, written as [21]:

$$\theta_z = \frac{180}{\pi} \arcsin(h/d) \tag{8}$$

where d denotes the distance from the BD to the UAV.

The term L_{LoS} and L_{NLoS} in (5) are the path-loss attenuation of LoS and NLoS, respectively, which are given by:

$$\begin{cases} L_{\text{LoS}} = 10\alpha_{\text{LoS}} \log(d) \\ L_{\text{NLoS}} = 10\alpha_{\text{NLoS}} \log(d) \end{cases} \tag{9}$$

where α_{LoS} and α_{NLoS} are the path-loss coefficients of the LoS and NLoS, respectively. Then, after combining (9), (7) and (5), we can transform the expression of g_{mix} as follows [21]:

$$g_{\text{mix}} = d^{-(\alpha_{\text{NLoS}} - P_{\text{LoS}} \cdot (\alpha_{\text{NLoS}} - \alpha_{\text{LoS}}))} = d^{-\chi} \tag{10}$$

where χ represents $\alpha_{\text{NLoS}} - P_{\text{LoS}} \cdot (\alpha_{\text{NLoS}} - \alpha_{\text{LoS}})$.

The small-scale fading in our network utilizes the Nakagami fading model, which is a general channel model. Let g_{c} characterize the gain of the Nakagami fading model. The term g_{c} follows a Gamma distribution with shape factor m [22], [23]. The corresponding probability density function (PDF) is described by [21], [23]:

$$f_{g_{\text{c}}}(x) = 2m^m x^{2m-1} \frac{\mathrm{e}^{\frac{-mx^2}{\Omega}}}{\Gamma(m)\Omega^m} \tag{11}$$

where Ω represents the mean value, m donates the Nakagamim fading parameter, and $\Gamma(m) = \int_0^\infty t^{m-1}\mathrm{e}^{-t}\mathrm{d}t$ is the standard Gamma function.

2.3 Backscatter Communications

The backscatter communication utilized is illustrated in Fig. 3 [24], [25]. The RF signals received by BDs play two roles: signal transmission and energy harvesting. Part of the signals is harvested to provide the energy for power circuits, while the remaining portion is used to transmit information [26]. When different bits need to be transmitted, the reflected signals can be modulated by the micro-controller module switching to various impedances to reflect signals with different amplitudes [27]. Let ρ represent the reflection coefficient of the BackCom. The reflection coefficient is the ratio of the reflected signals to the total received RF signals at BDs. We assume that P_{UAV} and P_{BD}^{r} are the transmitted power of the UAV and the received power of BDs respectively. Then, the reflected/transmitted power of BD, represented by $P_{\text{BD}}^{\text{ref}}$, can be expressed by:

$$P_{\text{BD}}^{\text{ref}} = \rho P_{\text{BD}}^{\text{r}} = \rho P_{\text{UAV}} G_{\text{d}} g_{\text{mix}} g_{\text{c}}. \tag{12}$$

Subsequently, we consider the energy harvesting scheme. Due to the TDMA scheme, each BD can only transmit data to the UAV during one slot, leaving the remaining non-transmission slots available for energy harvesting. Specifically, we let $E_{\text{BD}_{\text{e}}}^{T_{\text{c}}}$ represent the received energy stored in BDs during T_{c}. We then consider the energy harvesting conversion model. Conventional studies on UAV-assisted BackCom networks consider a linear energy harvesting model. However, the linear model cannot illustrate the nonlinearity caused by hardware constraints in practical energy harvesting circuits [28]. Therefore, following [11, 29–32], we consider a non-linear energy harvesting conversion model. Let $E_{\text{BD}_{\text{h}}}^{T_{\text{c}}}$ represent the harvested energy during T_{c}. Then, $E_{\text{BD}_{\text{h}}}^{T_{\text{c}}}$ can be given as follows [11, 28–32]:

$$E_{\text{BD}_{\text{h}}}^{T_{\text{c}}} = \frac{\Phi - E_{\max}^{\text{EH}} \Omega_{\text{EH}}}{1 - \Omega_{\text{EH}}}, \tag{13}$$

$$\Omega_{\text{EH}} = \frac{1}{1 + \mathrm{e}^{b_1 b_2}}, \quad \Phi = \frac{E_{\max}^{\text{EH}}}{1 + \mathrm{e}^{-b_1 (E_{\text{BD}_{\text{e}}}^{T_{\text{c}}} - b_2)}} \tag{14}$$

where $E_{\max}^{\text{EH}}$ represents the maximum power output, while parameters b_1 and b_2 are associated with the specific circuits used for energy harvesting.

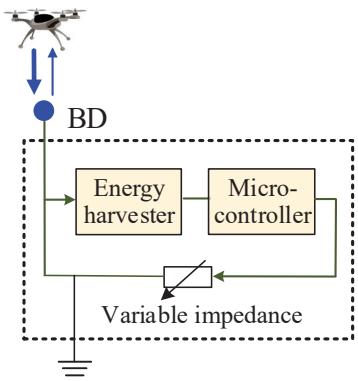

Fig. 3. Backscatter communications.

3. Altitude Range and Throughput

3.1 Altitude Range

The altitude range of the UAV can be assessed based on conditions for successful BackCom between the UAV and BDs. The successful establishment of communication links between a UAV and BDs relies on two key conditions: 1) BDs need to have adequate power for conducting BackCom, and 2) the UAV needs to effectively receive the BackCom signals, ensuring that the signal-to-noise ratio (SNR) at the UAV is higher than a certain communication threshold δ_0. These conditions are referred to as the "BackCom condition" and the "SNR condition", respectively. We first analyze these two conditions and then give the valid altitude range.

BackCom Condition

Based on our TDMA scheme and harvesting strategy mentioned in Sec. 2.1, the total energy received during the time period T_c for harvesting at the BD, denoted by $E_{\mathrm{BD_e}}^{\mathrm{T_c}}$, can be described as follows [20]:

$$\begin{aligned} E_{\mathrm{BD_e}}^{\mathrm{T_c}} =& (1-\rho)\cdot P_{\mathrm{BD}}^{\mathrm{r}}\cdot\frac{T_c}{N}+(N-1)\cdot P_{\mathrm{BD}}^{\mathrm{r}}\cdot\frac{T_c}{N} \\ =& \left(\frac{N-\rho}{N}\right)P_{\mathrm{UAV}}G_d\left(\frac{h}{\cos(\theta_d/2)}\right)^{-\chi}g_c T_c. \end{aligned} \tag{15}$$

Let η_e represent the minimum power required for circuit operation in BackCom. Thus, the BackCom of BDs can only be initiated on condition that the harvested energy $E_{\mathrm{BD_h}}^{\mathrm{T_c}}$ during T_c is greater than or equal to $\eta_e \cdot T_c/N$, written as [20]:

$$E_{\mathrm{BD_h}}^{\mathrm{T_c}} \geq \eta_e \cdot T_c/N. \tag{16}$$

By combining (16), (13), and (14), Equation (16) can be transformed as follows:

$$E_{\mathrm{BD_e}}^{\mathrm{T_c}} \geq -\frac{1}{b_1}\ln\left(\frac{E_{\max}^{\mathrm{EH}}(1+\exp(b_1 b_2))}{\frac{\eta_e T_c}{N(h)}\exp(b_1 b_2)+E_{\max}^{\mathrm{EH}}}-1\right)+b_2. \tag{17}$$

Let $C(h)$ represent the right-hand side of (17), i.e., $C(h) = -\frac{1}{b_1}\ln\left(\frac{E_{\max}^{\mathrm{EH}}(1+\exp(b_1 b_2))}{\frac{\eta_e T_c}{N(h)}\exp(b_1 b_2)+E_{\max}^{\mathrm{EH}}}-1\right)+b_2$. Subsequently, through the combination of (17), (15), (3)[1], (4), and (1), the new BackCom condition can be expressed as:

$$2\pi\lambda_{\mathrm{BD}}P_{\mathrm{UAV}}g_c T_c\phi_1 h^2 - \pi\lambda_{\mathrm{BD}}\phi_2 C(h)h^{2+\chi} - \frac{2\rho P_{\mathrm{UAV}}g_c T_c}{1-\cos(\theta_d/2)} \geq 0 \tag{18}$$

where ϕ_1 and ϕ_2 are functions relies on the variable of θ_d. $\phi_1 = \tan^2(\theta_d/2)/(1-\cos(\theta_d/2))$, and $\phi_2 = \tan^2(\theta_d/2)/\cos^{\chi}(\theta_d/2)$. Based on (18), the maximum altitude denoted as $h_{\max}^{\mathrm{BackC}}$ and the minimum altitude denoted as $h_{\min}^{\mathrm{BackC}}$ can be calculated using MATLAB tool.

SNR Condition

To ensure successful communications between the UAV and BDs, we need to consider the SNR condition: the SNR at the UAV is not below δ_0. In our channel model, we consider additive white Gaussian noise. Let σ^2 be the power of noise. The SNR of the received signal at the UAV represented by SNR_{UAV} can be written as:

$$SNR_{\mathrm{UAV}} = \frac{P_{\mathrm{BD}}^{\mathrm{ref}}G_d g_{\mathrm{mix}}g_c}{\sigma^2}. \tag{19}$$

After combining (19), (12), (10), and (1), Equation (19) can be given by:

$$\begin{aligned} SNR_{\mathrm{UAV}} =& \frac{\rho P_{\mathrm{UAV}}g_{\mathrm{mix}}^2 g_c^2}{\sigma^2}\left(\frac{2}{1-\cos(\theta_d/2)}\right)^2 \\ =& \frac{\rho P_{\mathrm{UAV}}d^{-2\chi}g_c^2}{\sigma^2}\left(\frac{2}{1-\cos(\theta_d/2)}\right)^2. \end{aligned} \tag{20}$$

We substitute d in (20) with $d_{\max}$ as defined in (3) (for similar reason given in footnote 1), and then integrate it with the condition $SNR_{\mathrm{UAV}} \geq \delta_0$ to yield the following equation:

$$h \leq \left(\frac{\rho P_{\mathrm{UAV}}}{\delta_0\sigma^2}\right)^{\frac{1}{2\chi}}\left(\frac{2}{1-\cos(\theta_d/2)}\right)^{\frac{1}{\chi}}\cos(\theta_d/2)g_c^{\frac{1}{\chi}}. \tag{21}$$

It is evident from (21) that the maximum altitude, determined by the SNR condition, is contingent on the variable g_c. Subsequently, upon obtaining the expected value of g_c, we can express the maximum altitude $h_{\max}^{\mathrm{SNR}}$ as follows:

$$h_{\max}^{\mathrm{SNR}} = \left(\frac{\rho P_{\mathrm{UAV}}}{\delta_0\sigma^2}\right)^{\frac{1}{2\chi}}\left(\frac{2}{1-\cos(\theta_d/2)}\right)^{\frac{1}{\chi}}\cos(\theta_d/2)\int_0^{\infty}x^{\frac{1}{\chi}}f_{g_c}(x)\mathrm{d}x \tag{22}$$

where $f_{g_c}(x)$ is derived as (11).

Valid Altitude Range

In UAV-assisted BackCom networks, the valid altitude range of the UAV not only depends on the inner communication restraints such as the BackCom condition and the SNR condition, but also relies on outer local environmental constraints and UAV regulations. For example, some limitation need to be considered on the minimum and maximum values of the altitude because of local environmental factors such as trees and buildings or laws/regulations. We assume that $h_{\min}^{\mathrm{out}}$ and $h_{\max}^{\mathrm{out}}$ denote the minimum altitude and maximum altitude based on the above-mentioned outer constraints/law/regulations, respectively. Then, the valid altitude range for the UAV can be formulated by:

[1]It is worth noting that we use $d_{\max}$ to replace the variable d in (15). This is because $d_{\max}$ is the maximum distance between the UAV and BDs within the coverage region of the UAV. In order to ensure all BDs in the coverage region of the UAV can have enough energy to conduct BackCom, we need to consider the maximum distance $d_{\max}$.

$$\begin{aligned} &h \in [h_{\min}^{\mathrm{UAV}}, h_{\max}^{\mathrm{UAV}}], \\ &h_{\min}^{\mathrm{UAV}} = \max\{h_{\min}^{\mathrm{BackC}}, h_{\min}^{\mathrm{out}}\}, \\ &h_{\max}^{\mathrm{UAV}} = \min\{h_{\max}^{\mathrm{BackC}}, h_{\max}^{\mathrm{SNR}}, h_{\max}^{\mathrm{out}}\} \end{aligned} \tag{23}$$

where both $h_{\min}^{\mathrm{BackC}}$ and $h_{\max}^{\mathrm{BackC}}$ can be given according to (18), and $h_{\max}^{\mathrm{SNR}}$ is obtained by (22).

The valid altitude range of UAVs in UAV-assisted BackCom networks is dependent on $h_{\min}^{\mathrm{BackC}}$, $h_{\max}^{\mathrm{BackC}}$, and $h_{\max}^{\mathrm{SNR}}$. It can be observed that from (18) (the formula to obtain $h_{\min}^{\mathrm{BackC}}$ and $h_{\max}^{\mathrm{BackC}}$) that the values of $h_{\min}^{\mathrm{BackC}}$ and $h_{\max}^{\mathrm{BackC}}$ are dependent on three parameters: the antenna beamwidth θ_{d}, the minimum power required for circuit operation η_{e}, and the density of λ_{BD}. In addition, from (22), we can find that $h_{\max}^{\mathrm{SNR}}$ is relies on the antenna beamwidth θ_{d}. These phenomenons indicate that the valid altitude of the UAV is dependent on the directional antenna of the UAV, the BackCom scheme of BD, and the distribution of BDs. Their specific relationship will be investigated in the next section.

3.2 Throughput

In order to calculate the total throughput within a unit time, let $\mathbb{T}_i^{\mathrm{T_c}}$ be the throughput from the UAV to the ith BD during T_{c} time period. Then, the total throughput in T_{c} time period, denoted by $\mathbb{T}_{\mathrm{total}}^{\mathrm{T_c}}$, can be expressed as:

$$\mathbb{T}_{\mathrm{total}}^{\mathrm{T_c}} = \sum_{i=1}^{N} \frac{T_{\mathrm{c}}}{N} \cdot \mathbb{T}_i^{\mathrm{T_c}}. \tag{24}$$

Subsequently, the total throughput $\mathbb{T}_{\mathrm{total}}$ within the unit time can be formulated as

$$\mathbb{T}_{\mathrm{total}} = \frac{\mathbb{T}_{\mathrm{total}}^{\mathrm{T_c}}}{T_{\mathrm{c}}} = \frac{1}{N} \sum_{i=1}^{N} \mathbb{T}_i^{\mathrm{T_c}} = \mathbb{E}_i[\mathbb{T}_i^{\mathrm{T_c}}] \tag{25}$$

where $\mathbb{E}_i[\mathbb{T}_i^{\mathrm{T_c}}]$ represents the mathematical expectation of $\mathbb{T}_i^{\mathrm{T_c}}$.

Let SNR_{UAV}^i be the SNR for the BackCom at the UAV from the ith BD, and d_i represent the distance from the UAV to the ith BD. Then, Equation (25) can be further formulated as:

$$\begin{aligned} \mathbb{T}_{\mathrm{total}} =& \mathbb{E}_i[B\log_2(1+SNR_{\mathrm{UAV}}^i)] \\ =& \mathbb{E}_{i,g_{\mathrm{c}}}\left[B\log_2\left(1+\frac{\rho P_{\mathrm{UAV}} d_i^{-2\chi} g_{\mathrm{c}}^2}{\sigma^2}\left(\frac{2}{1-\cos(\theta_{\mathrm{d}}/2)}\right)^2\right)\right] \\ =& \mathbb{E}_{i,g_{\mathrm{c}}}\left[B\log_2\left(1+\phi_3 d_i^{-2\chi} g_{\mathrm{c}}^2\right)\right] \end{aligned} \tag{26}$$

where $\phi_3 = \frac{\rho P_{\mathrm{UAV}}}{\sigma^2}\left(\frac{2}{1-\cos(\theta_{\mathrm{d}}/2)}\right)^2$, and B is defined as the bandwitdth of the BackCom between the UAV and BDs.

The term r_i is the radius from the ith BD to the coverage zone center of the UAV, where $r_i \in [0, h\tan(\theta_{\mathrm{d}}/2)]$. Accordingly, d_i in (26) can be written as:

$$d_i = (h^2 + r_i^2)^{1/2} \tag{27}$$

where the PDF of r_i can be given by [19]:

$$f_{r_i}(r) = \frac{2\pi r}{S} = \frac{2\pi r}{\pi h^2 \tan^2(\theta_{\mathrm{d}}/2)} = \frac{2r}{h^2\tan^2(\theta_{\mathrm{d}}/2)} \tag{28}$$

where S is derived in (2).

Then, Equation (26) can be expressed as the following:

$$\begin{aligned} \mathbb{T}_{\mathrm{total}} =& \mathbb{E}_{r_i,g_{\mathrm{c}}}\left[B\log_2\left(1+\phi_3(h^2+r_i^2)^{-\chi}g_{\mathrm{c}}^2\right)\right] \\ =& B\int_0^{h\tan(\frac{\theta_{\mathrm{d}}}{2})}\left(\int_0^{\infty}\log_2(1+\phi_3(h^2+r^2)^{-\chi}x^2)f_{g_{\mathrm{c}}}(x)\mathrm{d}x\right)f_{r_i}(r)\mathrm{d}r \end{aligned} \tag{29}$$

where $f_{r_i}(r)$ and $f_{g_{\mathrm{c}}}(x)$ are derived by (28) and (11), respectively.

According to (29), we can observe that the total throughput within a unit time is dependent on multiple key parameters such as the altitude of UAVs (h), the beamwidth of directional antennas (θ_{d}), the minimum power required for circuit operation in BackCom (η_{e}) (determine the valid altitude range of UAVs), and the density of BDs (λ_{BD}). Based on the expression given in (29), we can adjust the altitude of UAVs and the beamwidth of directional antennas to improve the throughput according to different network settings (with various η_{e} and λ_{BD}) in a given network environment.

4. Simulations

We perform simulations in MATLAB to validate our analytical model. Values of all parameters in the simulation are presented as follows: $P_{\mathrm{UAV}} = 10$ dBm, $\delta_0 = 5$ dB [24], $m = 2$ [21], $\Omega = 2$, $\mu_1 = 4.88$ [21], $\mu_2 = 0.429$ [21], $T_{\mathrm{c}} = 1$ s, $B = 1$ MHz [24], $b_1 = 150$ [29], $b_2 = 0.014$ [29], $E_{\max}^{\mathrm{EH}} = 24$ mW [29], $\sigma^2 = -60$ dBm [24], $\rho = 0.375$ [24][2], $h_{\min}^{\mathrm{out}} = 10$ m, and $h_{\max}^{\mathrm{out}} = 100$ m. In the subsequent figures, "ana" and "sim" denote outcomes from analysis and simulations, respectively. Each simulation outcome is obtained through Monte Carlo simulations involving an average of 2000 trials.

4.1 Altitude Range

Figures 4, 5, and 6 illustrate the altitude of the UAV with varied minimum power required for circuit operation (η_{e}), the directional antenna beamwidth of the UAV (θ_{d}), and the density of BDs (λ_{BD}), respectively, where the corresponding UAV altitude range is depicted in shadow. In these figures, the agreement of the analytical and simulation results verifies the precision of our analytical model.

[2]The term $\rho = 0.375$ is acquired by assuming equiprobable symbols in the case of binary constellations, and antenna impedances in the BackCom module are set to 0.5 and 0.75 [24].

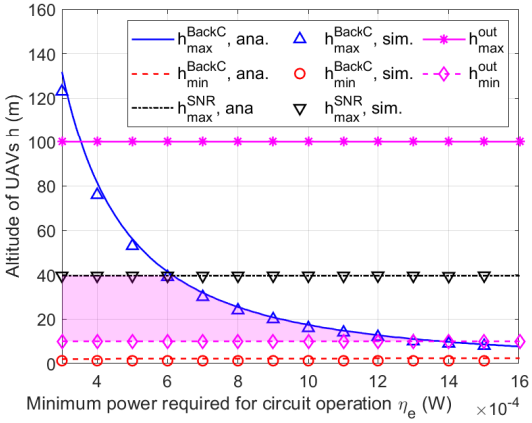

Fig. 4. The altitude range of the UAV (h) versus the minimum power required for circuit operation (η_e), where $\lambda_{BD} = 0.1/m^2$, $\theta_d = \pi/3$, $\alpha_{LoS} = 2.6$, and $\alpha_{NLoS} = 3$.

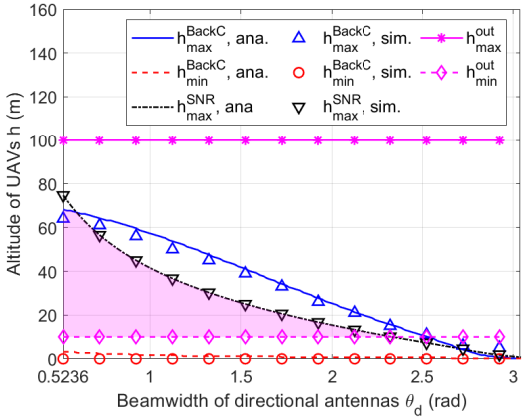

Fig. 5. The altitude range of the UAV (h) versus the beamwidth of directional antennas (θ_d), where $\eta_e = 0.001$ W, $\lambda_{BD} = 0.2/m^2$, $\alpha_{LoS} = 2.6$, and $\alpha_{NLoS} = 3$.

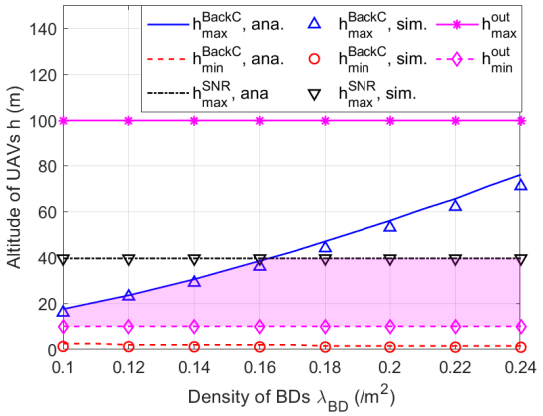

Fig. 6. The altitude range of the UAV (h) versus the density of BDs (λ_{BD}), where $\eta_e = 0.001$ W, $\theta_d = \pi/3$, $\alpha_{LoS} = 2.6$, and $\alpha_{NLoS} = 3$.

Figure 4 depicts the altitude range of the UAV (h) in relation to the minimum power required for circuit operation (η_e). In Fig. 4, when $\eta_e < 0.0006$ W, the maximum altitude maintains at a stable value with the increment of η_e. This is because the maximum altitude is restrained by h_{max}^{SNR}, while h_{max}^{SNR} is not associated with η_e; when $\eta_e > 0.0006$ W, the maximum altitude differs with varied η_e. The larger η_e leads to the narrower UAV altitude range. This is because the maximum altitude under BackCom condition (i.e., h_{max}^{BackC}) decreases with the increment of η_e, i.e., the larger η_e brings the greater energy demand for BackCom, resulting in the lower h_{max}^{BackC}. In addition, we can also find that when $\eta_e > 0.0014$ W, there is no suitable altitude for the UAV to collect data. Under these circumstances, we need to adjust other parameters such as increasing the UAV power to find valid altitude. From this figure, we can find that it is significant to investigate the altitude range to choose the proper UAV altitude in UAV-assisted BackCom networks.

Figure 5 illustrates the altitude range of the UAV (h) in relation to the beamwidth of directional antenna (θ_d). In Fig. 5, it shows that the maximum altitude varies with different beamwidth of directional antennas: both altitudes h_{max}^{BackC} and h_{max}^{SNR} increase as the beamwidth of directional antennas decreases. When the antenna beamwidth $\theta_d < 2.33$ (rad), the maximum altitude of the UAV is restrained by the maximum value of h_{max}^{BackC} and h_{max}^{SNR}; when the antenna beamwidth $\theta_d > 2.33$ (rad), there is no suitable altitude for the UAV to collect data. This is attributed to the narrower beamwidth resulting in the higher antenna gain, leading to increased harvested energy and SNR, and subsequently the higher maximum altitude. This observation emphasizes the significance of selecting the antenna beamwidth for directional UAV-assisted BackCom networks.

Figure 6 shows the relationship between the altitude range of the UAV (h) and the density of BDs (λ_{BD}). In Fig. 6, we can observe when the density $\lambda_{BD} < 0.16$, the altitude range changes as λ_{BD} varies: the maximum altitude of the UAV rises as λ_{BD} increases, and the maximum altitude of the UAV is restrained by h_{max}^{BackC}. This indicates that the altitude of the UAV is influenced by λ_{BD}. When the density $\lambda_{BD} > 0.16$, the maximum altitude of the UAV is a constant restrained by h_{max}^{SNR}. This is because h_{max}^{SNR} is independent of λ_{BD}. From Fig. 6, we can find that the altitude of the UAV needs to be adjusted based on the specific density values of BDs.

4.2 Throughput

Figures 7(a) and 7(b) depict the total throughput in unit time ($\mathbb{T}_{total}$) versus the altitude of UAVs (h), considering different path-loss coefficients of the LoS (α_{LoS}) and antenna beamwidths (θ_d), respectively. The consistency between the analytical and simulation results validates our analytical model's accuracy. We can observe from Fig. 7 that the total throughput in unit time decreases as the UAV altitude increases. This indicates that a higher-altitude UAV can cover a larger number of BDs for data collection, the total throughput in unit time still diminishes. This is because the increased altitude leads to the reduction of SNR, consequently yielding the lower average throughput within a specified time period and thereby resulting in the lower total throughput ($\mathbb{T}_{total} = \mathbb{E}_i[\mathbb{T}_i^{T_c}]$ as defined by (25)).

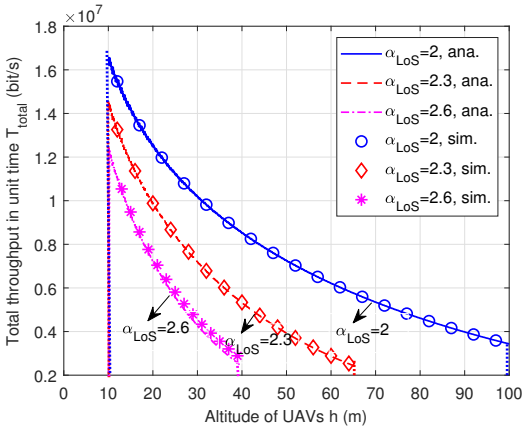

(a) The total throughput in unit time ($\mathbb{T}_{\text{total}}$) with varied path-loss coefficients of the LoS (α_{LoS}), where $\theta_{\text{d}} = \pi/3$

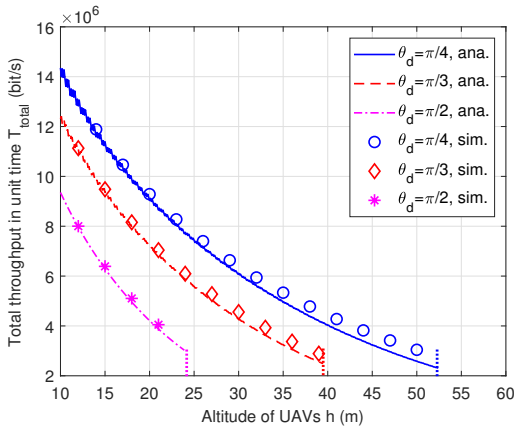

(b) The total throughput in unit time ($\mathbb{T}_{\text{total}}$) with varied antenna beamwidth (θ_{d}), where $\alpha_{\text{LoS}} = 2.6$

Fig. 7. The total throughput in unit time ($\mathbb{T}_{\text{total}}$) versus the altitude of UAVs (h). Other parameters: $\alpha_{\text{NLoS}} = 3$, $\lambda_{\text{BD}} = 0.2\,/\text{m}^2$ and $\eta_{\text{e}} = 0.001$ W.

Furthermore, in Fig. 7(a), we can find that the valid altitude of UAVs becomes narrower when the path-loss coefficient α_{LoS} increases. In addition, the larger path-loss coefficient α_{LoS} leads to the lower total throughput in unit time when given the same altitude of the UAVs. This indicates that we need to consider different environments when we choose the possible altitude for UAVs.

In addition, in Fig. 7(b), it can be observed that the total throughput in unit time increases when the antenna beamwidth decreases from $\pi/2$ to $\pi/4$ at a given UAV altitude. This implies that adjusting the beamwidth of directional antennas can enhance the total throughput in unit time.

5. Conclusions and Further Works

This paper analyzes the altitude range and total throughput in unit time of directional UAV-assisted BackCom networks by considering both BackCom condition and SNR condition. The accuracy of the analytical results is validated by simulations. The extensive simulations evaluate the impacts of key parameters (the minimum power required for circuit operation in BackCom, the beamwidth of directional antennas, and the density of BDs) on the valid altitude range or the throughput. Based on our analytical model and results, UAVs can set the proper UAV altitude and antenna beamwidth of directional antennas to ensure successful communications or improve the throughput.

Our further work will investigate the altitude range and the throughput in directional UAV-assisted BackCom networks based on the non-orthogonal multiple access (NOMA) since the NOMA technique is a key technique in both 5G and 6G.

Acknowledgments

This work was supported in part by the National Natural Science Foundation of China under Grant 62301563, in part by the Natural Science Foundation of Jiangsu Province under Grant BK20210490, in part by the Major Project of Natural Science Research of the Jiangsu Higher Education Institutions of China under Grant 21KJA520006, in part by the Xuzhou Science and Technology Plan Project under Grant KC21007.

References

[1] JIANG, T., ZHANG, Y., MA, W., et al. Backscatter communication meets practical battery-free internet of things: A survey and outlook. *IEEE Communications Surveys & Tutorials*, 2023, vol. 25, no. 3, p. 2021–2051. DOI: 10.1109/comst.2023.3278239

[2] REZAEI, F., GALAPPATHTHIGE, D., TELLAMBURA, C., et al. Coding techniques for backscatter communications - A contemporary survey. *IEEE Communications Surveys & Tutorials*, 2023, vol. 25, no. 2, p. 1020–1058. DOI: 10.1109/comst.2023.3259224

[3] JIANG, X., SHENG, M., ZHAO, N., et al. Outage analysis of UAV-aided networks with underlaid ambient backscatter communications. *IEEE Transactions on Wireless Communications*, 2023, vol. 22, no. 11, p. 7492–7505. DOI: 10.1109/TWC.2023.3251979

[4] TRAN, D.-H., CHATZINOTAS, S., OTTERSTEN, B. Throughput maximization for backscatter- and cache-assisted wireless powered UAV technology. *IEEE Transactions on Vehicular Technology*, 2022, vol. 71, no. 5, p. 5187–5202. DOI: 10.1109/tvt.2022.3155190

[5] YANG, H., YE, Y., CHU, X., et al. Energy efficiency maximization for UAV-enabled hybrid backscatter-harvest-then-transmit communications. *IEEE Transactions on Wireless Communications*, 2022, vol. 21, no. 5, p. 2876–2891. DOI: 10.1109/TWC.2021.3116509

[6] JIANG, X., SHENG, M., ZHAO, N., et al. UAV-assisted networks with underlaid ambient backscattering: Modeling and outage analysis. In *Proceedings of IEEE Global Communications Conference (GLOBECOM)*. Rio (Brazil), 2022, p. 4947–4952. DOI: 10.1109/globecom48099.2022.10000797

[7] HUA, M., YANG, L., LI, C., et al. Throughput maximization for UAV-aided backscatter communication networks. *IEEE Transactions on Communications*, 2020, vol. 68, no. 2, p. 1254–1270. DOI: 10.1109/tcomm.2019.2953641

[8] YANG, G., DAI, R., LIANG, Y.-C. Energy-efficient UAV backscatter communication with joint trajectory design and resource optimization. *IEEE Transactions on Wireless Communications*, 2021, vol. 20, no. 2, p. 926–941. DOI: 10.1109/TWC.2020.3029225

[9] TANG, G., LI, X., JI, H., et al. Optimization of trajectory scheduling and time allocation in UAV-assisted backscatter communication. In *Proceedings of IEEE International Conference on Communications Workshops (ICC Workshops)*. Montreal (Canada), 2021, p. 1–6. DOI: 10.1109/iccworkshops50388.2021.9473549

[10] AL-HOURANI, A., KANDEEPAN, S., LARDNER, S. Optimal LAP altitude for maximum coverage. *IEEE Wireless Communications Letters*, 2014, vol. 3, no. 6, p. 569–572. DOI: 10.1109/lwc.2014.2342736

[11] WANG, Q., ZHOU, Y., DAI, H.-N., et al. Performance on cluster backscatter communication networks with coupled interferences. *IEEE Internet of Things Journal*, 2022, vol. 9, no. 20, p. 20282–20294. DOI: 10.1109/JIOT.2022.3174002

[12] FARAJZADEH, A., ERCETIN, O., YANIKOMEROGLU, H. UAV data collection over NOMA backscatter networks: UAV altitude and trajectory optimization. In *IEEE International Conference on Communications (ICC)*. Shanghai (China), 2019, p. 1–7. DOI: 10.1109/ICC.2019.8761125

[13] VAEZI, M., AZARI, A., KHOSRAVIRAD, S. R., et al. Cellular, wide-area, and non-terrestrial IoT: A survey on 5G advances and the road towards 6G. *IEEE Communications Surveys & Tutorials*, 2022, vol. 24, no. 2, p. 1117–1174. DOI: 10.1109/comst.2022.3151028

[14] SCHWARZ, S., PRATSCHNER, S. Multiple antenna systems in mobile 6G: Directional channels and robust signal processing. *IEEE Communications Magazine*, 2023, vol. 61, no. 4, p. 64–70. DOI: 10.1109/mcom.001.2200258

[15] LIU, J., YU, J., NIYATO, D., et al. Covert ambient backscatter communications with multi-antenna tag. *IEEE Transactions on Wireless Communications*, 2023, vol. 22, no. 9, p. 6199–6212. DOI: 10.1109/TWC.2023.3240463

[16] WANG, X., YIGITLER, H., JANTTI, R. Gaining from multiple ambient sources: Signaling matrix for multi-antenna backscatter devices. *IEEE Wireless Communications Letters*, 2023, vol. 12, no. 3, p. 491–495. DOI: 10.1109/lwc.2022.3231907

[17] BALANIS, C. A. *Antenna Theory: Analysis and Design*. 3rd ed., New York: John Wiley & Sons, 2005. ISBN: 9781118642061

[18] WANG, Q., DAI, H.-N., ZHENG, Z., et al. On connectivity of wireless sensor networks with directional antennas. *Sensors*, 2017, vol. 17, no. 1, p. 1–22. DOI: 10.3390/s17010134

[19] WANG, Q., DAI, H.-N., GEORGIOU, O., et al. Connectivity of underlay cognitive radio networks with directional antennas. *IEEE Transactions on Vehicular Technology*, 2018, vol. 67, no. 8, p. 7003–7017. DOI: 10.1109/tvt.2018.2825379

[20] YANG, S., DENG, Y., TANG, X., et al. Energy efficiency optimization for UAV-assisted backscatter communications. *IEEE Communications Letters*, 2019, vol. 23, no. 11, p. 2041–2045. DOI: 10.1109/lcomm.2019.2931900

[21] LIU, Y., WANG, Q., DAI, H.-N., et al. UAV-assisted wireless backhaul networks: Connectivity analysis of uplink transmissions. *IEEE Transactions on Vehicular Technology*, 2023, vol. 72, no. 9, p. 12195–12207. DOI: 10.1109/tvt.2023.3268025

[22] KHAWAJA, W., GUVENC, I., MATOLAK, D. W., et al. A survey of air-to-ground propagation channel modeling for unmanned aerial vehicles. *IEEE Communications Surveys & Tutorials*, 2019, vol. 21, no. 3, p. 2361–2391. DOI: 10.1109/COMST.2019.2915069

[23] SIMON, M. K., ALOUINI, M.-S. *Digital Communication over Fading Channels*. New York: Wiley, 2004. ISBN: 9780471649533

[24] LU, X., JIANG, H., NIYATO, D., et al. Wireless-powered device-to-device communications with ambient backscattering: Performance modeling and analysis. *IEEE Transactions on Wireless Communications*, 2018, vol. 17, no. 3, p. 1528–1544. DOI: 10.1109/TWC.2017.2779857

[25] SHI, L., HU, R. Q., YE, Y., et al. Modeling and performance analysis for ambient backscattering underlaying cellular networks. *IEEE Transactions on Vehicular Technology*, 2020, vol. 69, no. 6, p. 6563–6577. DOI: 10.1109/tvt.2020.2984529

[26] LI, D. Backscatter communication powered by selective relaying. *IEEE Transactions on Vehicular Technology*, 2020, vol. 69, no. 11, p. 14037–14042. DOI: 10.1109/tvt.2020.3029340

[27] VAN HUYNH, N., HOANG, D. T., LU, X., et al. Ambient backscatter communications: A contemporary survey. *IEEE Communications Surveys & Tutorials*, 2018, vol. 20, no. 4, p. 2889–2922. DOI: 10.1109/comst.2018.2841964

[28] BOSHKOVSKA, E., NG, D. W. K., ZLATANOV, N., et al. Practical non-linear energy harvesting model and resource allocation for SWIPT systems. *IEEE Communications Letters*, 2015, vol. 19, no. 12, p. 2082–2085. DOI: 10.1109/LCOMM.2015.2478460

[29] MAO, Z., HU, F., WU, W., et al. Joint distributed beamforming and backscattering for UAV-assisted WPSNs. *IEEE Transactions on Wireless Communications*, 2023, vol. 22, no. 3, p. 1510–1522. DOI: 10.1109/TWC.2022.3204915

[30] SONG, X., CHIN, K. W. A novel hybrid access point channel access method for wireless-powered IoT networks. *IEEE Internet of Things Journal*, 2021, vol. 8, no. 15, p. 12329–12338. DOI: 10.1109/JIOT.2021.3063375

[31] ZARGARI, S., KHALILI, A., WU, Q., et al. Max-min fair energy-efficient beamforming design for intelligent reflecting surface-aided SWIPT systems with non-linear energy harvesting model. *IEEE Transactions on Vehicular Technology*, 2021, vol. 70, no. 6, p. 5848–5864. DOI: 10.1109/tvt.2021.3077477

[32] WANG, Q., ZHOU, Y., DAI, H.-N., et al. Modeling and analysis of finite-scale clustered backscatter communication networks. In *IEEE International Conference on Communications (ICC)*. Rome (Italy), 2023, p. 1456–1461. DOI: 10.1109/ICC45041.2023.10279058

About the Authors . . .

Zhaoyang WANG was born in Jiangsu province, China. He received his M.Sc. from Northeast Electric Power University in 2007. He is currently a lecturer at the School of Information Engineering, Xuzhou University of Technology. His research interests include the performance of wireless networks, computer networks, and UAV-assisted networks.

Qiu WANG (corresponding author) was born in Sichuan province, China. She received her M.Sc. and Ph.D. from Macau University of Science and Technology in 2014 and 2018, respectively. She is currently a lecturer at the School of Information Engineering, Xuzhou University of Technology. Her primary research interests include the performance of wireless networks, stochastic geometry, and UAV-assisted networks.

Xiangying DANG received her Ph.D. in Control Theory and Control Engineering from the China University of Mining and Technology in 2020. She is a Professor at the School of Information Engineering (School of Big Data), Xuzhou University of Technology. Her primary research interests encompass software engineering-based search, mutation testing and analysis, and wireless networks.